Nanocatalysts Assisted Growth of Diamond Films on Si by Hot Filament CVD

C. C. Teng,[*] F. C. Ku,[**] J. P. Deng,[***] S. F. Chien,*** C. M. Sung[**] and C. T. Lin[*]
[*]Department of Chemistry and Biochemistry,
Northern Illinois University, DeKalb, IL, USA, ctlin@niu,edu
[**]Kinik Company, Ying-Ko, Taipei, Taiwan, sung@kinik.com.tw
[***]Tamkang University, Tamsui, Taiwan, jpdeng@mail.tku.edu.tw

ABSTRACT

Four different catalysts, nano-Ni, diamond powder, mixture of nano-Ni/diamond powder, and ultrasonicated nanodiamond seed, were used to activate Si wafers for diamond film growth by hot filament CVD (HFCVD). Diamond crystals were shown to grow directly on both large diamond powder and small nanodiamond seed, but a better crystallinity of diamond film was observed on the ultrasonicated nanodiamond seeded Si substrate. On the other hand, nano-Ni nanocatalysts seem to promote the formation of amorphous and/or graphitic-like carbon at the initial growth of diamond films. The subsequent nucleation and growth of diamond crystals on top of the amorphous carbon layer were followed to generate the spherical diamond particles and clusters prior to coalescence into continuous diamond films. Moreover, the mixture of nano-Ni/diamond powder catalyst tend to promote the formation of a mixed of amorphous and crystallite diamond structures as characterized by TEM, Raman, and XRD techniques.

Keywords: Ni nanoparticle, nanodiamond seed, nanocatalyst, growth mechanism, diamond film, HFCVD

1 INTRODUCTION

Recently, nanocrystalline diamond films have been considered as the attractive materials for solid-state electronic applications; due to their hardness, thermal conductivity, electrical resistivity, UV transparency, etc. Different surface modification techniques, such as mechanical abrasion, ultrasonication and bias, have been used to enhance the initial nucleation density for diamond film growth [1]. In ultrasonication seeding, diamond powders and/or mixed with transition metal powders (Ni of 3~5 μm in size, Ti, Cu, Fe etc.) were processed as catalysts. However, the catalytic effect of Ni has been illustrated to inhibit CVD diamond nucleation and growth, though diamond might nucleate and grow on the amorphous carbon or graphitic interlayer initially formed on Ni in a low pressure methane-hydrogen environment [2-5]. For this reason, Ni nanoparticles were widely reported for synthesis of carbon nanotube (CNT) because the graphitic layer covering Ni particles of proper size in nanoscale would transform into CNT by CVD under a controlled temperature [6,7]. Under these conditions, CNT and diamond can be selectively grown on Ni coated and diamond powder abraded Si substrates [8]. Therefore, the better understanding of the detailed chemistry of diamond film growth assisted by Ni is essential to the better control of CVD diamond film or CNT growth in relation to the growth of initial species, chemical mechanisms and transformations to the final crystalline phase. In this paper, we employed four different catalysts, nano-Ni, diamond powder (250 ~ 350 nm), mixture of nano-Ni/diamond powder, and ultrasonicated nanodiamond (50 nm) seed, on Si wafers to investigate diamond film growth by HFCVD method. A growth mechanism is suggested to explain the effect of Ni nanoparticles on the initial growth stage of CVD diamond film formation.

2 EXPERIMENTAL

2.1 Preparation of Nanocatalysts

Nano-Ni nanocatalysts Nano-Ni nanocatalysts were prepared by a chemical reduction method and stabilized in ethylene glycol (EG) solutions containing poly(vinylpyrrolidone) (PVP) polymer stabilizers. First, a 10mL of 10mM $NaH_2PO_2 \cdot H_2O$ (sodium hypophosphite, J. T. Baker 3740) in an EG solution and a 10mL of 4mM $NiSO_4 \cdot 6H_2O$ (nickel (II) sulfate hexahydrate, Fisher N73-100) in an EG solution were freshly prepared, and then well mixed by a magnetic stirrer for 30 minutes. Second, about 0.74 wt% of PVP (polyvinylpyrrolidone, SIGMA-ALDRICH 437190-500G, $M_w \approx 1{,}300{,}000$ (LS)) powder was added into the $NaH_2PO_2 \cdot H_2O/NiSO_4 \cdot 6H_2O$/EG solution and mixed for at least 1.5 hour. Third, the final solution was heated under microwave (2.45 GHz, 900W) for 3 minutes until the color of the solution changed from light green to black brown, indicating the formation of nano-Ni nanoparticle in solutions.

Diamond powders solution First, about 0.37wt% of PVP was added into a 46g EG solution and mixed with a magnetic stirrer for at least 1.5 hour. Second, 1wt% of fluorosurfactant (FS, Dupont FS-510) was added into the PVP/EG solution and mixed for 30 minutes. Third, 0.005wt% of diamond powder (SP-DP MapleCanada Group) was added into the FS/PVP/EG solution and well dispersed by a sonicationb dismembrator (Fisher Scientific Model-100) with 15W power for 30 seconds.

NSTI-Nanotech 2008, www.nsti.org, ISBN 978-1-4200-8503-7 Vol. 1

2.2 Deposition of Diamond Films by HFCVD

The polished (100) Si substrates were pretreated with either (a) nanodiamond seeds, ND (4~50 nm, Carbo-Tec Dynaget M3D) by ultrasonication, (b) diamond powders, NDP (250~350 nm, SP-DP MapleCanada Group), (c) nano-Ni nanoparticles or (d) a mixture of nano-Ni and NDP. The surface modification processes, (b), (c) and (d) were done by spin-coating (Photo-resist spinner EC101D-R485, Headway Res. Inc.). The pretreated Si substrates were used for diamond films deposition by HFCVD system (Sp3 Inc., Model 500). The deposition pressure was controlled at 18~20 Torr, containing a gas mixture of 2.3 vol% methane (99.995% purity) and hydrogen (99.95% purity) under a flow rate of 3000 sccm. The distance between the tungsten (W) filament and Si substrates was adjusted at 10 mm. The W filament temperature was controlled at 2000-2200 °C. The temperature of Si substrates was about 650~700°C in the seeding stage and about 800-850°C in the growing stage. In this work, an initial nucleation time of 1.5 hrs and a total deposition time of 48 hrs were employed.

2.3 Characterization Methods

A dynamic light scattering (DLS) goniometer equipped with a HeNe laser at 630 nm (Brookhaven Instruments, Model BI-200SM) was used to characterize the size and size distribution of Ni nanoparticle solutions. The diamond films were analyzed by X-ray powder diffraction measurements (XRD, Rigaku Corp., Model MiniFlex). The lattice structures were examined for the front surface diamond film (front-side) and also the interface between diamond film and Si substrate (backside). Renishaw Raman Scattering Noodles System 2000, equipped with a microscope and a HeNe red (632.8 nm) excitation laser, was used to examine the molecular properties and quality of diamond films from both the front and backsides. Scanning electron microscopy (SEM, JEOL JSM-5600) micrographs were taken to illustrate the surface morphology of diamond films on Si substrates. Atomic force microscopy (AFM, Quesant Q-scope 350) measurements were scanned for the surface pretreated Si substrates and also the front-side and backside of diamond films. Plan-view Transmission electron microscopy (TEM, JEOL, JSM-1200EX II) pictures were taken to identify the possible growing structures and/or species for the formation of diamond films.

3 RESULTS AND DISCUSSIONS

3.1 Size Distribution of Nano-Ni Catalysts with PVP in EG by DLS and AFM

DLS measurements gave a mean diameter of around 50 nm for both 1 mM and 2 mM of nano-Ni catalysts with 0.37 wt% PVP in EG solutions. The AFM pictures for the spin-coated nano-Ni on Si substrates were also shown to have the particle sizes of around 50 ~ 70 nm. (Both DLS and AFM figures are not shown here)

3.2 XRD Patterns of Diamond Films

Figure 1 shows XRD patterns of the front-side diamond films (catalyzed by ND – blue, nano-Ni – red, NDP - pink, and a mixture of nano-Ni/NDP – brown), which are labeled as CVDD-ND, CVDD-Ni, CVDD-NDP, and CVDD-NDP-Ni, respectively. The XRD spectra display three characteristic 2θ peaks around 44.3, 75.6 and 91.8 degrees, which may be assigned to <111>, <220> and <311> lattice planes of diamond crystal, respectively. In Figure 2(b), the XRD patterns for the backsides (B-CVDD) of diamond films are also presented, where only a small bump at 2θ around 75.5 degree (or <220> plane) of diamond crystal has started to come out at the initial growth stage. On the backside of diamond film, both <111> and <311> were not observed. This observation may suggest the possible phase transition from the nondiamond to diamond <111> faces during the growth of diamond films. From the crystallographic diagram, the dominant growth in <110> (or its parallel <220> face) should give diamond crystals of pyramidal <111> facets.[12] Thus, the backside shoulder band of 2θ around 75.8 degree is probably resulted from the stacking faults along <220> direction. All XRD peaks observed in Figure 1 are quite broad (FWHM 0.3 ~ 0.5 degrees in 2θ), suggesting the formation of small diamond crystals. The observed XRD peaks displayed a peak shift of 2θ about 0.3~0.4 degrees relative to the theoretical positions that indicates the inhomogeneous stresses existed in diamond films. A peak splitting for <111> peak at 2θ = 44.3 degrees was observed for nano-Ni assisted diamond films as shown in Figure 1(a). The reason is not yet known, but it may be resulted from the lattice mismatching for the growth of diamond crystals on nano-Ni particle-like catalysts.

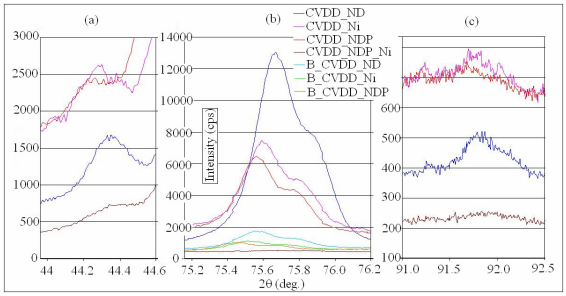

Figure 1: XRD of diamond films: (a) D<111>, (b) D<220>, front & backside and (c) D<311> lattice planes

3.3 Raman Spectra of Diamond Films

Figure 2 shows Raman spectra of diamond films catalyzed by ND (blue), nano-Ni (pink), and NDP (green). Both front and backsides of diamond films were examined, where the backside film served as the film growth at the

initial stage. In all cases, the crystalline diamond peak at 1332 cm^{-1} is only weakly observed (the inserted in Figure 2), suggesting the % and size of diamond in film composition is low and small. However, an amorphous phase starts to form at the initial stage as observed by a small broad band at 1520 cm^{-1} on the backside. This is then transformed to give the diamond structure as displayed by a small peak around 1334 cm^{-1} on the front side.

All spectra showed an intense band at 2270 cm^{-1} and a shoulder band at 2800 cm^{-1}, which have been attributed to several origins: (1) a photoluminescence peak or a color center due to silicon defects in the growth of diamond films [10,11], and (2) the overtone Raman band of a short conjugation chain of trans-polyacetylene (t-PA), which may grow around the grain boundaries of diamond films [12-16]. The origin (2) is preferred since these Raman bands have also been observed for the diamond films grown on non-silicon substrates [17]. Moreover, in Figure 2, the intensity of 2270 cm^{-1} peak is even stronger on the front than on the backsides of diamond films grown on Si by HFCVD. This indicates that the 2270 cm^{-1} peak is not due the substrate defects, but the t-PA formed around the grain boundaries of small (or nano) diamonds. It is worthwhile to mention, the backside diamond film catalyzed by nano-Ni gives the lowest peak intensity of Raman band at 2270 cm^{-1}, indicating the production of t-PA is low in the initial growth of diamond phase on nano-Ni catalysts. This may be resulted from the catalytic dehydrogenation effects that inhibit the formation of t-PA.

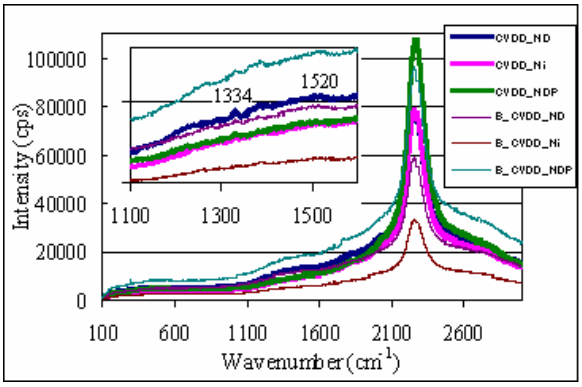

Figure 2: Raman spectra of diamond films

3.4 TEM Study of Diamond Films

TEM pictures are very informative for identifying the initial growth species of diamond films as shown in Figure 3 on (a) ND, (b) nano-Ni, (c) NDP, and (d) nano-Ni/NDP mixture. For diamond film grown on diamond seed/powder, such as pictures (a), (c) & (d-1), the nanocrystalline diamond clusters were shown to be the dominant structures of several overlapping hexagonal forms. Picture d-1, in particular, a well-defined crystalline structure is clearly seen. On the surface of nano-Ni catalyst, however, some short tube-like structures (picture b-2) and a 2-5 nm thin graphitic-like layer (picture d-2) were shown to nucleate on nano-Ni catalysts of various sizes, which may be identified in picture b-2 (10-15 nm), b-3 and d-2 (30 nm). An interesting observation in picture b-1 should be mentioned, where diamond crystals seem to be formed on amorphous/graphitic-like interlayers initially grown on nano-Ni catalysts without diamond seeding. Moreover, in picture d-3, nano-Ni catalysts clusters were shown to embed in amorphous phase of diamond films. The observed tube-like and graphitic-like layer forms on nano-Ni surface may lead us to speculate that those are the initial growth species before a transformation to amorphous phase and then to the crystalline diamond structures.

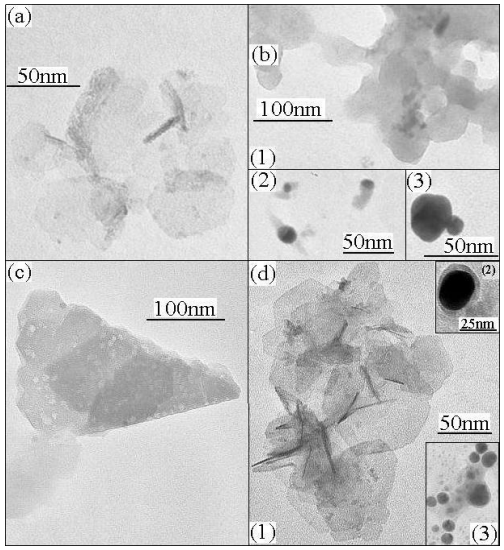

Figure 3: TEM of diamond films (a) CVDD-ND, (b) CVDD-Ni, (c) CVDD-NDP, (d) CVDD-NDP-Ni

3.5 SEM and AFM Study of Diamond Films

SEM pictures of diamond films grown on the pretreated Si substrates (a - nano-Ni and b - NDP) are shown in Figure 4. The pyramidal <111> facet of diamond crystals are clearly observed in the inserted pictures under high resolution. It is interesting to point out that the continuous polycrystalline diamond films were formed by the coalescence of the spherical cauliflower-like microcrystalline diamond particles about 20 μm in size. These diamond structures are particularly striking as seen in Figure 4(b), and their coalescing boundaries of the resulting diamond films are pointed by arrows. The formation of spherical cauliflower-like microcrystalline diamond particles may result from the isotropic nucleation and growth of nanodiamond crystals on large nanodiamond powders. On the surface of nano-Ni catalyst, however, amorphous carbon (or graphitic-like layer as shown in TEM) may be formed initially at lower temperature of 700°C and followed by the nucleation of nanodiamond

NSTI-Nanotech 2008, www.nsti.org, ISBN 978-1-4200-8503-7 Vol. 1

crystals and then transformed to the spherical cauliflower-like microcrystalline diamond particles.

The continuous faceted diamond films grown on different pretreated Si substrates are quite similar at first glance. The detailed examination shows that the diamond films grown on ND surface gave the most crystalline diamond particles as demonstrated in XRD analysis. The diamond films grown on nano-Ni catalysts seem to have the smaller size and less crystalline diamond particles as shown in Figure 4(a). This can be viewed from the right-bottom inserts of Figure 4 (a) & (b), the diamond crystals on the surface of the single spherical cauliflower-like microcrystalline diamond particle assisted by nano-Ni have less crystallinity than those seeded with NDP and ND.

The smaller diamond particles grown on nano-Ni (a), as compared to those on ND, can also be seen in AFM scans in Figure 5. The surface roughness (Rt) of diamond films were measured as 1.552 μm and 0.905 μm for Figure 5 (a) and (b), respectively. A 40% reduction in surface roughness for diamond film grown on nano-Ni is a surprise and quite significant.

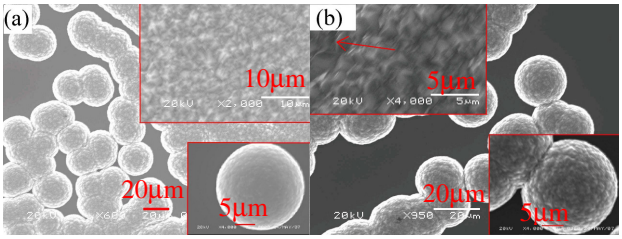

Figure 4: SEM of diamond films (a) CVDD-Ni (b) CVDD-NDP

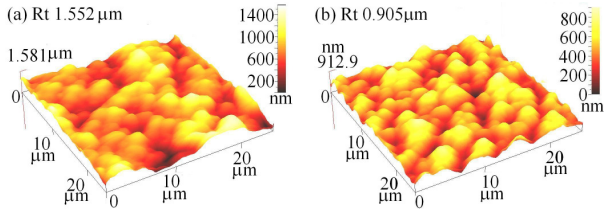

Figure5: AFM of diamond films (a) CVDD-ND and (b) CVDD-Ni

4 CONCLUSIONS

We have successfully demonstrated the diamond films grown on ND, nano-Ni, NDP, and nano-Ni/NDP mixture by HFCVD. The initial growth seems to have the <220> (or <110>) facets and then leads to diamond crystals of pyramidal <111> facets as shown in XRD. The Raman spectral band at 2270 cm^{-1} has been verified to originate from the short chain t-PA formed around the grain boundaries of small (or nano) diamonds. The SEM and TEM results indicated that diamond crystals were grown directly on both large NDP sites and small ND seeds, but latter displayed a better crystallinity of diamond film. It was clearly illustrated that nano-Ni nanocatalysts can promote the formation of amorphous and/or graphitic-like carbon phases at the initial growth of diamond films, and the subsequent nucleation and growth of diamond crystals on top of the amorphous carbon layer to generate the spherical diamond particles and clusters prior to coalescence into continuous diamond films. Moreover, a 40% reduction in surface roughness for diamond film grown on nano-Ni is a surprise and quite significant.

ACKNOWLEDGMENT

This work was supported by Kinik Company, Taiwan and Institute for Nano Science, Engineering and Technology, NIU. The technical assistances from Dr. Laurence Lurio, Dr. Haji-Shiekh and Dr. Chong Zheng are greatly appreciated.

REFERENCES

[1] Y. Chakk, R. Brener and A. Hoffman, Appl. Phys. Lett. 66, 2819, 1995.; Diamond Relat. Mater. 5, 286, 1996.; Diamond Relat. Mater. 6, 681, 1997.
[2] D. N. Belton and S. J. Schieg, J. Appl. Phys. 66, 4223, 1989.
[3] P. C. Yang, W. Zhu and J. T. Glass, J. Mater. Res. 9, 1063, 1994.; J. Mater. Res. 8, 1773, 1993.
[4] E. Johansson, P. Skytt, J.-O. Carlsson, N. Wassdahl and J. Nordgren, J. Appl. Phys. 79, 7248, 1996.
[5] W. Zhu, P. C. Yang, J. T. Glass, Appl. Phys. Lett. 63, 1640, 1993.
[6] M. Yudasaka, R. Kikuchi, T. Matsui, Y. Ohki and S. Yoshimura, Appl. Phys. Lett. 67, 2477, 1995.
[7] M. Mauger, V. T. Binh, A. Levesque and D. Guillot Phys. Lett. 85, 305, 2004.
[8] Q. Yang, C. Xiao, W. Chen and A. Hirose, Diamond Relat. Mater. 13, 433, 2004.
[9] M. N. R. Ashfold, P. W. May and C. A. Rego, Chem. Soc. Rev. 23, 21, 1994.
[10] J. Birrell, J. E. Gerbi, O. Auciello, J. M. Gibson, J. Johson and J. A. Carlisle, Diamond Relat. Mater. 14, 86, 2005.
[11] D. V. Musale, S. R. Sainkar, S. T. Kshirsagar, Diamond Relat. Mater. 11, 75, 2002
[12] I. I. Vlasov, V. G. Ralchenko, E. Goovaerts, A. V. Savelie and M. V. Kanzyuba, Phys. Stat. Sol. (a) 203, 3028, 2006.
[13] Sh. Michaelson, O. Ternyak and A. Hoffman, Appl. Phys. Lett. 89, 131918, 2006.
[14] D. Roy, Z. H. Barber and T. W. Clyne, J. Appl. Phys. 91, 6085, 2002.
[15] A. C. Ferrari and J. Robertson, Phys. Rev. B. 63, 121405-1, 2001
[16] T. López-Ríos, É. Sandré, S. Leclercq and É. Sauvain, Phys. Rev. Lett. 76, 4935, 1996.
[17] L.-T. S. Lin, G. Popovici, M. A. Prelas, S. Khasawinah and T. Sung, J. Chem. Vap. Dep. 3, 102, 1994.